View metadata, citation and similar papers at core.ac.uk
brought to you by CORE
provided by Universität München: Elektronischen Publikationen

Cite this: *CrystEngComm*, 2011, **13**, 5559

www.rsc.org/crystengcomm

PAPER

Self-assembly of melem on Ag(111)—emergence of porous structures based on amino-heptazine hydrogen bonds

Johanna Eichhorn,*[a] Stefan Schlögl,[a] Bettina V. Lotsch,[b] Wolfgang Schnick,[b] Wolfgang M. Heckl[ac] and Markus Lackinger*[ac]

Received 21st March 2011, Accepted 9th May 2011
DOI: 10.1039/c1ce05342f

Downloaded by Ludwig Maximilians Universitaet Muenchen on 28 January 2013
Published on 22 June 2011 on http://pubs.rsc.org | doi:10.1039/C1CE05342F

Self-assembly of melem on Ag(111) as studied by Scanning-Tunneling-Microscopy (STM) in ultra-high vacuum revealed a great structural variety. In total, five porous and two densely packed monolayer polymorphs were observed. All structures are stabilized by intermolecular hydrogen bonds, where melem–melem arrangements are based on very few basic motifs. Six out of seven polymorphs can be described by a unified concept.

Porous surface-supported supramolecular monolayers have gained substantial interest,[1] due to potential applications as host-networks for the inclusion of guests or even as organic templates for growth of size selected metal nanoparticles. In the design of porous organic networks, crystal engineers very often take advantage of the relative strength and directionality of hydrogen bonds, whereby porous structures can become favoured over densely packed polymorphs. In this respect the carboxylic acid moiety is an abundant functional group,[2] because in most cases it forms double $O_{hydroxyl}$–H···$O_{carbonyl}$ hydrogen bonds in a self-complementary manner. The high formation probability of cyclic double hydrogen bonds between two carboxylic acid groups has allowed for a certain degree of predictability of the final structure and aided in the rational design of building blocks in "supramolecular retro-synthesis". Yet, competing interactions in molecular self-assembly of carboxylic acids can also promote alternative hydrogen bond patterns.[3] Surface-confined hydrogen bonded networks of carboxylic acids have so far only been demonstrated on fairly unreactive substrates such as graphite or noble metal surfaces. On more reactive substrates carboxylic acid groups have a strong tendency to deprotonate and the resulting carboxylate group preferably forms bonds with the substrate or takes part in metal-coordination bonds, when coordination centers become available. For instance, trimesic acid (TMA, 1,3,5-tricarboxybenzene) self-assembles into porous hydrogen bonded flower and chickenwire structures on graphite,[4,5] whereas on Cu(100)[6] and even on Au(111) under electrochemical control,[7] TMA adsorbs upright and is anchored through a carboxylate-surface bond. Also the tricarboxylic acid 1,3,5-benzenetribenzoic acid, a larger analogue of TMA also with threefold symmetry, self-assembles into porous networks at the solution–graphite interface,[8] and on Ag(111) for room temperature deposition under UHV conditions.[9] However, upon annealing to 320 K and 420 K respectively, two phase transitions resulted in more densely packed structures and were explained by a stepwise deprotonation of all carboxylic groups.

So far a great variety of 2D porous networks with different pore sizes, shapes, and arrangements have been demonstrated, hence the next rewarding step would be the identification and realization of applications. In this respect a very intriguing and promising application idea envisages porous networks as growth template for size selected, surface supported metal nanoparticles. While these metal nanoparticles might be relevant for heterogeneous catalysis, it is well established that the supporting substrate can also contribute to their size dependent catalytic activity. Gold nanoparticles on TiO_2 are a prominent example thereof.[10] With this application in mind, a next step in this direction would be to design and study molecular building blocks which bear the potential to self-assemble into porous molecular networks on more reactive substrates. The aim of this study was to conceive supramolecular building blocks equipped with less reactive functional groups which are suitable for self-assembly into hydrogen bonded porous networks on more reactive surfaces. To this end, we targeted the combination of amino groups as hydrogen bond donors and heterocyclic aromatic nitrogen atoms as hydrogen bond acceptors.

Melamine (1,3,5-triazine-2,4,6-triamine, Fig. 1(a)) is an archetypical building block in this respect, whose homomeric two-dimensional self-assembly has already been studied on Au (111)[11] and Ag(111).[9,12] For both substrates two different porous melamine structures were reported, while on Au(111) an additional close packed polymorph was observed. All melamine monolayer structures are stabilized by the targeted N_{amino}–H··· $N_{triazine}$ hydrogen bonds. However, the pore sizes of melamine networks around ~1.0 nm are comparatively small,[12] and even

[a]*Department of Physics, TUM School of Education, Technical University Munich, Schellingstrasse 33, 80333 Munich, Germany. E-mail: johanna.eichhorn@ lrz.uni-muenchen.de*
[b]*Department of Chemistry and Center for Nanoscience (CeNS), Ludwig Maximilian University, Butenandtstr. 5-13, 81377, Munich, Germany*
[c]*Deutsches Museum, Museumsinsel 1, 80538 Munich, Germany*

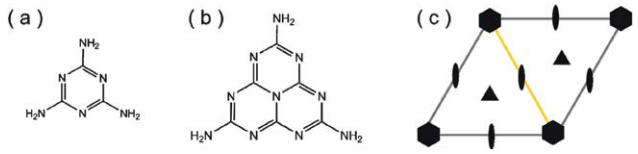

Fig. 1 Comparison of the molecular structures of (a) melamine and (b) melem; (c) arrangement of symmetry elements within a unit cell for the plane symmetry group *p*6.

Downloaded by Ludwig Maximilians Universitaet Muenchen on 28 January 2013
Published on 22 June 2011 on http://pubs.rsc.org | doi:10.1039/C1CE05342F

inclusion of further melamine molecules as guests within the pores already causes a substantial distortion of the network. The pore size can be increased dramatically by combining melamine with perylene tetra-carboxylic di-imide (PTCDI) as has been demonstrated both under UHV conditions[13,14] and at the liquid–solid interface.[15] In the corresponding heteromeric hexagonal monolayer melamine acts as vortices, while PTCDI molecules interconnect the vortices by means of triple hydrogen bonds. Yet, the preparation of heteromeric systems features stoichiometry and deposition sequence as further degrees of freedom and is much more challenging.

A further effective strategy for increasing the pore diameter is to rely on isotopological networks, where the length of a spacer group or molecule is increased, whereas the underlying blueprint of the structure remains similar. This fundamental principle of crystal engineering has been proven to work in the reticular synthesis of Metal–Organic-Framework (MOF) bulk crystals,[16] but could also be transferred to 2D networks on surfaces, as exemplified by metal-coordination networks based on dicarbonitrile–polyphenyl linker molecules,[17] hydrogen bonded networks of tricarboxylic acids,[2] and heteromeric self-assembly of melamine and the homologous series of fatty acids.[18]

Following the proposed approach, starting from melamine (*cf.* Fig. 1(a) for structure), we did not increase the length of a linear spacer, but the size of the molecular core from triazine (C_3N_3) to heptazine (C_6N_7), whereby the symmetric substitution with three amino groups (NH_2) and therefore the three-fold symmetry are retained. Self-assembly of the resulting compound melem (*cf.* Fig. 1(b) for structure) is anticipated to bear similarities with melamine self-assembly with regard to intermolecular hydrogen bonds. On the other hand, the intermolecular bond motifs of the larger compound melem are expected to feature greater versatility and the overall stability of the networks will additionally benefit from the enhanced molecule–surface interaction. In order to study melem self-assembly, Ag(111) surface was chosen as a substrate, representing an intermediate test bed for a more reactive metal surface.

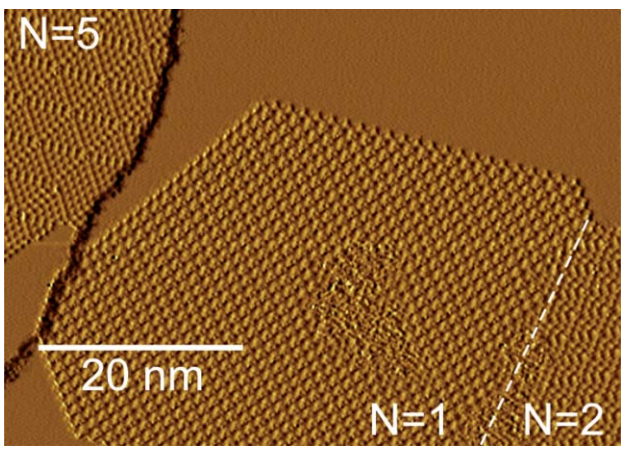

Fig. 2 Overview STM topograph (gradient) illustrating the co-existence of three different melem structures ($U = 1.26$ V, $I = 39$ pA). The dashed line in the lower left corner marks a domain boundary, and domains are labelled with their respective *N* value (*vide infra*).

Experimental

All experiments were carried out under ultra-high vacuum (UHV) conditions with a base pressure of 3.0×10^{-10} mbar. Ag(111) single crystal surfaces were prepared by successive cycles of Ar^+-ion sputtering and subsequent radiative annealing at 823 K. Melem was synthesised by thermal condensation of melamine,[19–21] and deposited from a home-built Knudsen cell[22] with a crucible temperature of 573 K onto the Ag(111) surface held at room temperature. Samples were characterized *in situ* by Scanning-Tunneling-Microscopy with a VT-STM from Omicron driven by a SPM100 control electronics from RHK. All measurements were conducted at room temperature using electrochemically etched tungsten tips, post-processed in UHV by electron-beam annealing. STM topographs were acquired in the constant-current mode of operation and images were processed by line-wise levelling only, if not indicated otherwise.

Results and discussion

Melem (2,5,8-triamino-1,3,4,6,7,9,9*b*-heptaazaphenalene) is a triply amino substituted heptazine (C_6N_7) ring. The molecule is essentially planar, has a threefold symmetry, and possesses an equilateral triangular footprint. Each baseline of the melem triangle features a D–A–A–D arrangement of hydrogen bond donors (D: NH_2) and acceptors (A: $N_{heptazine}$). Self-assembly of melem on Ag(111) as studied by STM is extremely versatile and revealed a great variety of long range ordered structures. Even though identical preparation protocols were used in numerous experimental runs, self-assembly yielded a variety of different, mostly co-existing melem polymorphs. An STM overview topograph illustrating the co-existence of three different melem structures is depicted in Fig. 2. In total up to seven different structures emerged, representative STM topographs of each observed polymorph are reproduced in Fig. 3(a)–(g). Among those, five melem monolayer polymorphs are porous and two are densely packed. Unit cell parameters, molecular area densities, and number of melem molecules per unit cell are summarized in Table 1. In all structures melem adsorbs planar, *i.e.* with the heptazine ring parallel to the surface. Melem is very suitable for STM-based self-assembly studies, because its size and even more so its characteristic triangular footprint allow us to infer the mutual position and azimuthal orientation of adjacent melem molecules. From the relative arrangement of interconnected melem molecules it becomes possible to deduce intermolecular bond motifs. In the following, we will first describe the porous and densely packed polymorphs, and then infer and analyze the underlying intermolecular hydrogen bond patterns.

 This journal is © The Royal Society of Chemistry 2011

Downloaded by Ludwig Maximilians Universitaet Muenchen on 28 January 2013
Published on 22 June 2011 on http://pubs.rsc.org | doi:10.1039/C1CE05342F

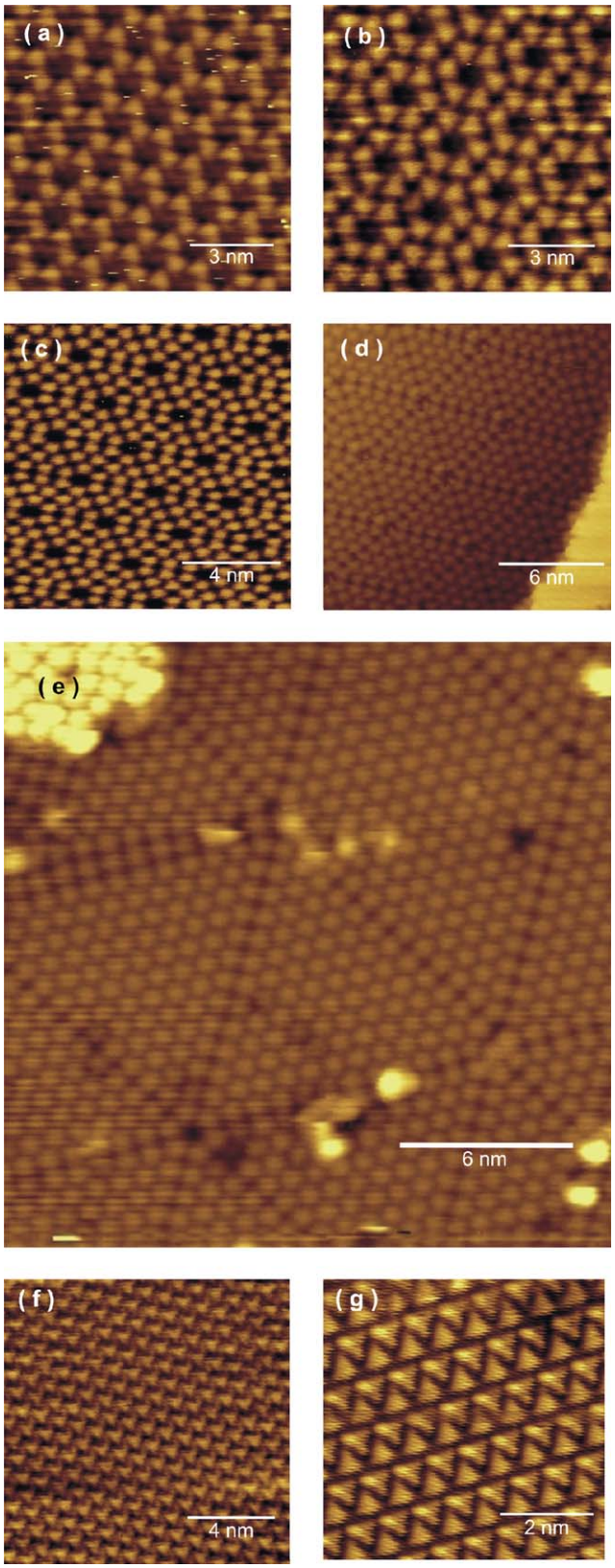

Fig. 3 High resolution STM topographs of all observed melem monolayer polymorphs on Ag(111) and tunneling parameters: (a) $N = 1$ (0.42 V, 45 pA), (b) $N = 2$ (1.01 V, 48.30 pA), (c) $N = 3$ (0.91 V, 74 pA), (d) $N = 5$ (1.26 V, 40 pA), (e) $N = 12$ (2.23 V, 1.07 pA), (f) trigonal densely packed polymorph (0.04 V, 75 pA), and (g) densely packed row structure (0.16 V, 97 pA).

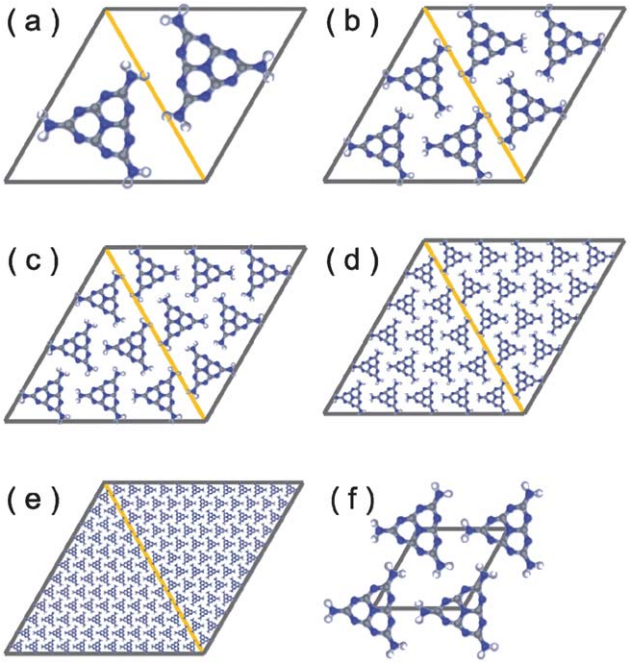

Fig. 4 Tentative models of the systematic series of melem polymorphs on Ag(111); for each polymorph the arrangement of melem molecules in one unit cell is shown. (a) $N = 1$, (b) $N = 2$, (c) $N = 3$, (d) $N = 5$, (e) $N = 12$, and (f) $N \rightarrow \infty$.

Table 1 Summary of crystallographic parameters of the observed melem polymorphs

Structure	Lattice parameter/nm		Packing density/ molecules per nm^2	Molecules per unit cell
	Experimental	Theoretical eqn (1)		
$N \rightarrow \infty$	0.9 ± 0.1	—	1.43	1
Densely packed row structure	$a = 0.75 \pm 0.1$ $b = 1.45 \pm 0.1$	—	2.13	2
$N = 1$	1.45 ± 0.1	1.45	1.10	2
$N = 2$	2.4 ± 0.1	2.35	1.20	6
$N = 3$	3.12 ± 0.1	3.25	1.42	12
$N = 5$	4.9 ± 0.1	5.05	1.44	30
$N = 12$	10.54 ± 0.1	11.4	1.62	156

Owing to their lone pair, nitrogen atoms in supramolecular building blocks can act either as hydrogen bond acceptors or as electron rich ligands for metal-coordination. However, on Ag(111) without additional supply of reactive extrinsic coordination centers comparable compounds form only intermolecular hydrogen bonds. Recent examples include terphenyl-4,4″-dicarbonitrile which assembles into a densely packed structure that is stabilized by N···H–C hydrogen bonds with phenyl hydrogen

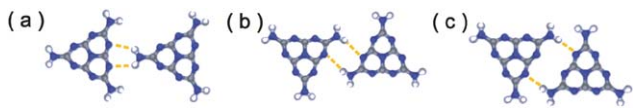

Fig. 5 Basic melem–melem binding motifs: (a) head-to-tail, (b) side-by-side, and (c) alternative side-by-side. The dashed lines indicate $N_{heptazine}\cdots H–N_{amino}$ hydrogen bonds.

Downloaded by Ludwig Maximilians Universitaet Muenchen on 28 January 2013
Published on 22 June 2011 on http://pubs.rsc.org | doi:10.1039/C1CE05342F

atoms.[23] *N*,*N*-Diphenyloxalic amide self-assembles into a chain structure based on N–H···O hydrogen bonds.[24]

Apparently, intrinsic Ag adatoms are not reactive enough to coordinate supramolecular building blocks through their nitrogen atoms. Since in the present study contrast features that hint towards coordinating Ag atoms have never been observed and the experimental intermolecular bond distances are consistent with a mere hydrogen bond scenario, formation of metal-coordination bonds can be excluded.

All porous polymorphs are hexagonal and belong to the chiral plane symmetry group *p*6. In each polymorph the pores feature a similar size (~0.8 nm inner van der Waals diameter), while the experimental interpore spacing, *i.e.* the lattice parameter, varies from 1.45 nm up to 10.5 nm. From the STM topographs it is evident that each pore is bordered by six melem molecules, but also a more in-depth analysis of the intermolecular hydrogen bond motifs becomes possible. With increasing lattice parameter of the porous structures the number of melem molecules per unit cell increases.

Besides the porous polymorphs two densely packed polymorphs were also observed. One of these is a relatively simple trigonal structure with one molecule per unit cell, while the second densely packed polymorph features two molecules per unit cell.

Tentative models of all structures based on the STM data are depicted in Fig. 4 and 7. Although the number of melem polymorphs is comparatively large, all porous structures can be condensed into a systematic series. Each porous polymorph belongs to the plane symmetry group *p*6 (*cf.* Fig. 1(c) for unit cell structure), with the sixfold rotation points centered at the pore. In each half of the unit cell (equilateral triangle) melem molecules adopt similar azimuthal orientation and are arranged in a trigonal densely packed structure. On each side where those triangular halves of the unit cells adjoin, a clearly visible seam (*cf.* Fig. 4(d) and (e)) indicates a different type of intermolecular melem–melem bond. The porous polymorphs can also be classified by the number N of melem molecules countable along the direct connection between two adjacent pores. In our experiments, porous polymorphs with $N = 1$, 2, 3, 5, and 12 were observed. Interestingly, only two different intermolecular hydrogen bond patterns account for the structural versatility of the five porous polymorphs. The two basic intermolecular melem–melem bonds are denoted as head-to-tail and side-by-side. Different mutual arrangements of two hydrogen bonded melem molecules were simulated by molecular mechanics (MM), results are depicted in Fig. 5. In the head-to-head arrangement (*cf.* Fig. 5(a)) the center-to-center distance of melem is ~0.92 nm, while in the side-by-side arrangement (*cf.* Fig. 5(b)) the center-to-center distance amounts to ~0.82 nm. Both basic hydrogen bond patterns feature two equivalent cyclic N_{amino}–H···$N_{heptazine}$ intermolecular hydrogen bonds. In the head-to-tail motif both hydrogen atoms of the same amino group bind to two adjacent heterocyclic nitrogen atoms of the heptazine ring through two parallel hydrogen bonds. Since this bond pattern requires two adjacent hydrogen bond acceptors, an equivalent hydrogen bond arrangement is not possible for the smaller analogue melamine. In the side-by-side arrangement one amino group and one heterocyclic nitrogen atom of each melem molecule form the double hydrogen bonds. Side-by-side was also identified as a preferred binding motif in the 3D crystal structure of melem[25] and is comparable to a similar intermolecular bond pattern of the smaller analogue melamine.[11,14,26] The head-to-tail arrangement features mirror symmetry, while the side-by-side arrangement is two-fold symmetric and chiral. Melem by itself is a non-chiral molecule and even remains non-chiral after adsorption on Ag (111), *i.e.* melem is also non-prochiral. Due to the chirality of the side-by-side hydrogen bond motif, however, each structure which includes this motif becomes chiral. For instance, the arrangement of six melem molecules bordering one pore is based on the side-by-side motif, and thus chiral. A single dimer is already chiral, and resulting six-membered rings can have a clockwise or counterclockwise arrangement. High resolution STM topographs of both enantiomeric melem arrangements around the pore for the $N = 1$ polymorph are presented in Fig. 6, along with the corresponding right- and left-handed models of the melem hexamer. Right- and left-handed forms of the supramolecular arrangement are energetically equivalent, and hence observed with equal probability.

In the structurally simplest porous polymorph for $N = 1$ melem molecules are exclusively interconnected side-by-side, where each melem molecule binds to three next nearest neighbours on each of its baselines. According to the unit cell structure of *p*6, melem molecules must be centered at the threefold rotational points. Consequently, their mutual distance obeys a fixed relation to the lattice parameter a: $d_{melem–melem} = a/\sqrt{3}$, yielding an experimental value $d_{melem–melem}$ of 1.45 nm/$\sqrt{3}$ = 0.84 nm. This value is very close to the MM results for the side-by-side arrangement depicted in Fig. 5(b). In contrast, the conceivable alternative side-by-side arrangement shown in Fig. 5(c) yields a smaller $d_{melem–melem} = 0.74$ nm, and the corresponding lattice parameter would only account to 1.28 nm, *i.e.* would be smaller than the experimental value. Also the angle of 28.5° between one melem baseline and the unit cell vector of the side-by-side motif in Fig. 5(b) is in better agreement with the experimental value of 28 ± 2°. Accordingly, we propose the side-by-side arrangement of Fig. 5(b) as intermolecular bond scheme in the porous polymorphs.

For the porous polymorphs with $N > 1$ a second hydrogen bond motif is required. As shown in the structural models, melem molecules in each half of the unit cells are exclusively interconnected in the head-to-tail arrangement, whereas at the three boundaries of the unit cell halves the side-by-side arrangement is prevalent. According to the *p*6 plane symmetry group, both halves of the unit cell are related by a two-fold rotational symmetry with the symmetry point at the center of the shorter diagonal (*cf.* Fig. 1(c)). This two-fold symmetry reflects the symmetry of the overall arrangement of molecules in the unit cell, but also the symmetry of the side-by-side arrangement. The six

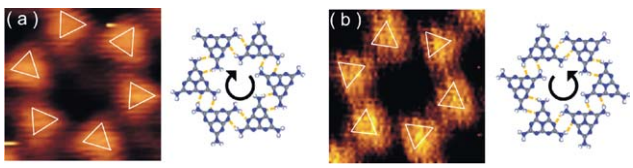

Fig. 6 STM topographs and corresponding models of chiral melem hexamers based on the side-by-side arrangement (a) clockwise and (b) counter-clockwise.

 This journal is © The Royal Society of Chemistry 2011

Downloaded by Ludwig Maximilians Universitaet Muenchen on 28 January 2013
Published on 22 June 2011 on http://pubs.rsc.org | doi:10.1039/C1CE05342F

melem molecules which form the pores at the corners of the unit cell are all interconnected side-by-side. Comparable, internally hydrogen bonded hexamers were also observed for homomeric self-assembly of melamine on Au(111),[11] but also as structural motif in heteromeric self-assembly of melamine and fatty acids.[18]

Starting from the simplest porous polymorph with only two molecules per unit cell and $N = 1$, the next element of the series can be obtained by introducing one more melem molecule in the direction along the lattice parameter in a head-to-tail arrangement. Accordingly, the lattice parameter increases in increments of 0.9 nm, *i.e.* by the center-to-center distance of the head-to-tail arrangement from one element of the series to the next. The lattice parameter a obeys the following equation:

$$a = 1.45\ \text{nm} + 0.9\ \text{nm} \times (N - 1) = 0.55\ \text{nm} + 0.9\ \text{nm} \times N \quad (1)$$

However, when N increases by 1 not only one melem molecule is added to the unit cell, but a row of melem molecules running parallel to the shorter diagonal. Since the number of melem molecules in this additional row increases with increments of 1, the number of molecules per unit cell as a function of N corresponds to:

$$\text{melem per unit cell} = 2\sum_{i=1}^{N} i = N(N+1) \quad (2)$$

From eqn (1) the unit cell area can be deduced as a function of N, and combination with eqn (2) yields the N dependence of the molecular area density:

$$\text{packing density} = \frac{2}{\sqrt{3}} \frac{N^2 + N}{(0.55\ \text{nm})^2 + 0.99\ \text{nm}^2 \times N + 0.81\ \text{nm}^2 \times N^2} \quad (3)$$

From eqn (3) one can infer that the molecular area density, and hence the packing density, increases monotonically with increasing N and the area density approaches a constant value of 1.43 molecules per nm^2 for $N \rightarrow \infty$. This is obvious since each unit cell of all polymorphs contains only one pore with fixed dimension, while the unit cell area increases monotonically with N. In principle the intermolecular hydrogen bonds do not impose any restriction on the values of N, and any integer number should be possible. Why experiments yielded only distinct values of N is not clear at this point and a possible influence of the substrate through epitaxial relations cannot be ruled out. Yet observation of polymorphs with $N = 12$ and accordingly 156 melem molecules per unit cell indicates extensibility of this systematic series up to very large unit cells. On the other hand, dislocations, *i.e.* additional or missing rows in one half of the unit cell in this structure, point towards a predisposition for defects for high N structures.

Similarly, systematic series of porous polymorphs with constant pore sizes but increasing lattice parameters, number of molecules per unit cell, and packing densities have already been observed for TMA on Au(111)[4,27] and 1,3,5-trikis(4′-carboxylphenyl)-2,4,6-trikis(4′-*tert*-butylphenyl)-benzene (HPB) on Au(111).[28] In accord with the melem results presented here, the systematic series of TMA networks is equally based on only two different intermolecular hydrogen bond patterns and two different azimuthal orientations of molecules.

The emergence of specific TMA polymorphs was dependent on the surface coverage, where higher coverages yielded more densely packed polymorphs with higher N value. For TMA, neither coexistence of polymorphs nor emergence of structures with large, but finite N, were reported. In contrast to TMA, for melem on Ag(111) structural control, *i.e.* deliberate and exclusive preparation of a specific polymorph could not be achieved by variation of experimentally accessible preparation parameters as surface coverage, deposition rate, or surface temperature. This distinct deviation from the TMA results is exemplified in Fig. 2 by the co-existence of three different melem structures, as observed even for submonolayer coverage. Furthermore, for TMA only the densely packed structure for $N \rightarrow \infty$ was observed, whereas melem self-assembly yielded two different densely packed polymorphs.

Polymorphism is also abundant in monolayer self-assembly at the liquid–solid interface,[3,5,8] and has likewise been observed for nitrogen-containing building blocks. For instance, oligopyridines yield different hydrogen bonded networks, where all structures are based on C–H···N hydrogen bonds.[29] Albeit probably not fully understood, at the liquid–solid interface structural control of monolayers can be accomplished by the choice of solvent, concentration, and temperature.[30,31]

A tentative model of the less complex trigonal densely packed polymorph with one molecule per unit cell is shown in Fig. 4(f). Intermolecular hydrogen bonds in this structure are exclusively based on the head-to-tail arrangement. Since in this hydrogen bond motif both molecules adopt the same azimuthal orientation, the trigonal densely packed structure contains only one molecule per unit cell. The mirror symmetry of the head-to-tail arrangement also results in the more symmetric *p3m*1 plane symmetry group. The lattice parameter of 0.9 nm of the trigonal densely packed polymorph is equal to the center-to-center distance in the melem head-to-tail arrangement. It is noteworthy that this densely packed polymorph can also be enqueued in the series of porous polymorphs as limiting case for $N \rightarrow \infty$. Since the unit cell becomes infinitely large, the side-by-side bonding motif, which is only prevalent at the boundaries and at the shorter diagonal of the unit cell of the porous polymorphs, does not occur anymore.

The second densely packed polymorph features a row like structure with two molecules per unit cell. Each row is comprised of melem molecules with alternating azimuthal orientations, where the baselines of the melem footprints are aligned parallel to the row direction. The monolayer structure consists of a dense packing of parallel rows, and melem molecules adjoin with parallel baselines of their triangular footprints. The tentative model of the structure including the unit cell and the hydrogen bond pattern is depicted in Fig. 7. The two melem molecules in the unit cell are rotated by 180° with respect to each other. Within the rows melem molecules are interconnected by the alternative side-by-side arrangement as illustrated in Fig. 5(c), where the amino groups do not interact with the heterocyclic nitrogen atoms next to the involved amino groups, but with the heterocyclic nitrogen atom next to the other amino group. The hydrogen bond pattern between the rows bears similarities with the regular side-by-side arrangement, however, the side of the melem molecules facing the boundaries between rows forms two side-by-side bonds with two melem molecules. This arrangement results in a geometrically slightly different, but still comparable, side-by-side motif.

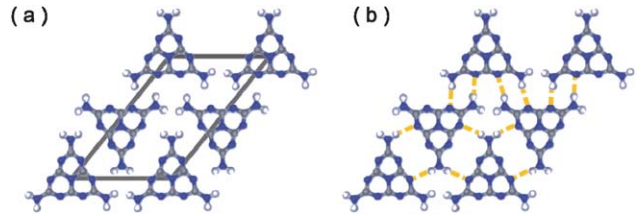

Fig. 7 Tentative model of (a) the unit cell and (b) the hydrogen bond pattern of the densely packed row polymorph with two melem molecules per unit cell.

For melamine a rather similar densely packed polymorph was reported which is also based on two different side-by-side arrangements.[11] Also a densely packed melem monolayer structure was previously observed by electrochemical STM on Au (111).[32] Although the reported structure also features two molecules per unit cell, the melem–melem arrangements are based on the two different binding motifs prevalent in the porous polymorphs of the present study, *i.e.* head-to-tail and side-by-side (*cf.* Fig. 5(a) and (b)). In summary the intermolecular hydrogen bonds in the more complex densely packed polymorph are still based on N_{amino}–H···$N_{heptazine}$, yet the underlying melem–melem arrangements are different from those in the systematic series of polymorphs.

Summary and outlook

In summary, we have shown that two-dimensional self-assembly of melem on Ag(111) is very versatile and yields a great structural variety of hydrogen bonded networks. In all structures melem molecules adsorb planar and are interconnected by N_{amino}–H···$N_{heptazine}$ hydrogen bonds. All structures except for one densely packed polymorph can be described as elements of a systematic series of structures, where the number N of melem molecules along the connection between adjacent pores increases in increments of one. Only two different intermolecular melem–melem hydrogen bond arrangements, denoted as side-by-side and head-to-tail, account for the observed versatility of porous two-dimensional melem structures. The higher porous polymorphs with $N =]1, \infty[$ feature both intermolecular bonding schemes, whereas both the trigonal densely packed polymorph ($N \rightarrow \infty$) and the simplest porous polymorph ($N = 1$) rely exclusively on the head-to-tail and side-by-side arrangement, respectively. Although the more complex densely packed polymorph is comprised of slightly different melem–melem arrangements, it is still stabilized by N_{amino}–H···$N_{heptazine}$ hydrogen bonds.

Polymorphism is abundant in surface-confined two-dimensional self-assembly and its origins are poorly understood. Commonly, the energetic equivalence of various structures on the scale of thermal energy contributes to the emergence of different polymorphs. In this respect increased structural versatility is expected for compounds with larger organic backbone like melem as opposed to melamine. The reason is that for larger compounds the molecule–substrate interaction increases, while the contribution of intermolecular hydrogen bonds to the overall binding energy remains about similar. Thus, the delicate balance between molecule–molecule and molecule–substrate interactions changes, and optimization of hydrogen bonds is not the only and probably not the decisive criterion for structure selection anymore. In addition, larger molecules allow for various other interactions, as seen for melem in the possibility of an alternative side-by-side and head-to-tail arrangement. Both contributions promote polymorphism.

For monolayer self-assembly at the liquid–solid interface, the influence of concentration and solvent is understood at a level which allows deliberate preparation of a distinct monolayer polymorph. However, for monolayers at the liquid–solid interface the relation between preparation parameters and monolayer structure is less well studied. In this regard nucleation and growth studies are very desirable. For the presented series of porous melem monolayers, being able to target a specific monolayer would be highly beneficial. All porous polymorphs feature similar pore size, but variable interpore spacing. Using these porous polymorphs as growth template for metal nanoparticles would thus allow tuning the spacing between nanoparticles with sub-nanometre precision in order to study distance-dependent effects. On the other hand, self-assembled melem monolayers might be promising precursor structures for the surface mediated polymerization into carbonitride polymers.[20]

Acknowledgements

Financial support by the Nanosystems-Initiative-Munich (NIM) cluster of excellence and the Elitenetzwerk Bayern is gratefully acknowledged for funding St. S.

Notes and references

1 T. Kudernac, S. B. Lei, J. A. A. W. Elemans and S. De Feyter, *Chem. Soc. Rev.*, 2009, **38**, 402–421.
2 M. Lackinger and W. M. Heckl, *Langmuir*, 2009, **25**, 11307–11321.
3 J. F. Dienstmaier, K. Mahata, H. Walch, W. M. Heckl, M. Schmittel and M. Lackinger, *Langmuir*, 2010, **26**, 10708–10716.
4 S. Griessl, M. Lackinger, M. Edelwirth, M. Hietschold and W. M. Heckl, *Single Mol.*, 2002, **3**, 25–31.
5 M. Lackinger, S. Griessl, W. A. Heckl, M. Hietschold and G. W. Flynn, *Langmuir*, 2005, **21**, 4984–4988.
6 A. Dmitriev, N. Lin, J. Weckesser, J. V. Barth and K. Kern, *J. Phys. Chem. B*, 2002, **106**, 6907–6912.
7 Z. Li, B. Han, L. J. Wan and T. Wandlowski, *Langmuir*, 2005, **21**, 6915–6928.
8 L. Kampschulte, M. Lackinger, A. K. Maier, R. S. K. Kishore, S. Griessl, M. Schmittel and W. M. Heckl, *J. Phys. Chem. B*, 2006, **110**, 10829–10836.
9 M. Ruben, D. Payer, A. Landa, A. Comisso, C. Gattinoni, N. Lin, J. P. Collin, J. P. Sauvage, A. De Vita and K. Kern, *J. Am. Chem. Soc.*, 2006, **128**, 15644–15651.
10 D. Matthey, J. G. Wang, S. Wendt, J. Matthiesen, R. Schaub, E. Laegsgaard, B. Hammer and F. Besenbacher, *Science*, 2007, **315**, 1692–1696.
11 F. Silly, A. Q. Shaw, M. R. Castell, G. A. D. Briggs, M. Mura, N. Martsinovich and L. Kantorovich, *J. Phys. Chem. C*, 2008, **112**, 11476–11480.
12 C. H. Schmitz, J. Ikonomov and M. Sokolowski, *Surf. Sci.*, 2011, **605**, 1–6.
13 J. A. Theobald, N. S. Oxtoby, M. A. Phillips, N. R. Champness and P. H. Beton, *Nature*, 2003, **424**, 1029–1031.
14 L. M. A. Perdigao, E. W. Perkins, J. Ma, P. A. Staniec, B. L. Rogers, N. R. Champness and P. H. Beton, *J. Phys. Chem. B*, 2006, **110**, 12539–12542.
15 R. Madueno, M. T. Raisanen, C. Silien and M. Buck, *Nature*, 2008, **454**, 618–621.
16 M. Eddaoudi, J. Kim, N. Rosi, D. Vodak, J. Wachter, M. O'Keeffe and O. M. Yaghi, *Science*, 2002, **295**, 469–472.
17 U. Schlickum, R. Decker, F. Klappenberger, G. Zoppellaro, S. Klyatskaya, M. Ruben, I. Silanes, A. Arnau, K. Kern, H. Brune and J. V. Barth, *Nano Lett.*, 2007, **7**, 3813–3817.

Downloaded by Ludwig Maximilians Universitaet Muenchen on 28 January 2013
Published on 22 June 2011 on http://pubs.rsc.org | doi:10.1039/C1CE05342F

 This journal is © The Royal Society of Chemistry 2011

18 H. Walch, A. K. Maier, W. M. Heckl and M. Lackinger, *J. Phys. Chem. C*, 2009, **113**, 1014–1019.
19 A. Sattler, S. Pagano, M. Zeuner, A. Zurawski, D. Gunzelmann, J. Senker, K. Müller-Buschbaum and W. Schnick, *Chem.–Eur. J.*, 2009, **15**, 13161–13170.
20 B. V. Lotsch and W. Schnick, *Chem. Mater.*, 2005, **17**, 3976–3982.
21 B. Jürgens, E. Irran, J. Senker, P. Kroll, H. Müller and W. Schnick, *J. Am. Chem. Soc.*, 2003, **125**, 10288–10300.
22 R. Gutzler, W. M. Heckl and M. Lackinger, *Rev. Sci. Instrum.*, 2010, **81**, 015108.
23 U. Schlickum, R. Decker, F. Klappenberger, G. Zoppellaro, S. Klyatskaya, W. Auwarter, S. Neppl, K. Kern, H. Brune, M. Ruben and J. V. Barth, *J. Am. Chem. Soc.*, 2008, **130**, 11778–11782.
24 F. Klappenberger, M. E. Canas-Ventura, S. Clair, S. Pons, U. Schlickum, Z. R. Qu, T. Strunskus, A. Comisso, C. Woll, H. Brune, K. Kern, A. De Vita, M. Ruben and J. V. Barth, *ChemPhysChem*, 2008, **9**, 2522–2530.
25 A. Sattler and W. Schnick, *Z. Anorg. Allg. Chem.*, 2006, **632**, 238–242.
26 M. Mura, N. Martsinovich and L. Kantorovich, *Nanotechnology*, 2008, **19**, 465704.
27 Y. C. Ye, W. Sun, Y. F. Wang, X. Shao, X. G. Xu, F. Cheng, J. L. Li and K. Wu, *J. Phys. Chem. C*, 2007, **111**, 10138–10141.
28 W. D. Xiao, X. L. Feng, P. Ruffieux, O. Groning, K. Müllen and R. Fasel, *J. Am. Chem. Soc.*, 2008, **130**, 8910–8912.
29 C. Meier, M. Roos, D. Kunzel, A. Breitruck, H. E. Hoster, K. Landfester, A. Gross, R. J. Behm and U. Ziener, *J. Phys. Chem. C*, 2010, **114**, 1268–1277.
30 S. B. Lei, K. Tahara, F. C. De Schryver, M. Van der Auweraer, Y. Tobe and S. De Feyter, *Angew. Chem., Int. Ed.*, 2008, **47**, 2964–2968.
31 R. Gutzler, T. Sirtl, J. F. Dienstmaier, K. Mahata, W. M. Heckl, M. Schmittel and M. Lackinger, *J. Am. Chem. Soc.*, 2010, **132**, 5084–5090.
32 T. Uemura, M. Aono, T. Komatsu and M. Kunitake, *Langmuir*, 2011, **27**, 1336–1340.

Published on 22 June 2011 on http://pubs.rsc.org | doi:10.1039/C1CE05342F
Downloaded by Ludwig Maximilians Universitaet Muenchen on 28 January 2013